Energy cascade and scaling in supersonic isothermal turbulence

Alexei G. Kritsuk[1]†, Rick Wagner[2] and Michael L. Norman[1,2]

[1]Department of Physics and Center for Astrophysics and Space Sciences, University of California, San Diego, MC 0424, 9500 Gilman Drive, La Jolla, CA 92093-0424, USA

[2]San Diego Supercomputer Center, University of California, San Diego, MC 0505, 10100 Hopkins Drive, La Jolla, CA 92093-0505, USA

(Draft version 11 July 2013)

Supersonic turbulence plays an important role in a number of extreme astrophysical and terrestrial environments, yet its understanding remains rudimentary. We use data from a three-dimensional simulation of supersonic isothermal turbulence to reconstruct an exact fourth-order relation derived analytically from the Navier–Stokes equations (Galtier and Banerjee, *Phys. Rev. Lett.*, vol. 107, 2011, p. 134501). Our analysis supports a Kolmogorov-like inertial energy cascade in supersonic turbulence previously discussed on a phenomenological level. We show that two compressible analogues of the four-fifths law exist describing fifth- and fourth-order correlations, but only the fourth-order relation remains 'universal' in a wide range of Mach numbers from incompressible to highly compressible regimes. A new approximate relation valid in the strongly supersonic regime is derived and verified. We also briefly discuss the origin of bottleneck bumps in simulations of compressible turbulence.

Key words: compressible turbulence, turbulence simulation, turbulence theory, turbulent flows

1. Introduction

Supersonic turbulence is believed to play a key role in a wide range of extreme astrophysical and terrestrial environments; for example, regulating star formation in molecular clouds (Hennebelle & Falgarone 2012), feeding supermassive black holes (Hobbs *et al.* 2011), creating clumpy structure in hot winds from Wolf-Rayet stars (Moffat & Robert 1994), controlling air entrainment in high-pressure volcanic eruptions (Ogden *et al.* 2008), and affecting fuel mixing and combustion efficiency in scramjets (Ingenito & Bruno 2010).

Compared to incompressible turbulence, highly compressible turbulent flows are more complex due to nonlinear coupling of the velocity, density and pressure fields. Shock waves and vortex sheets change the topology of intermittent dissipative structures in supersonic turbulence (Pan *et al.* 2009). A 'universal' scaling of the mass-weighted velocity $\boldsymbol{v} \equiv \rho^{1/3}\boldsymbol{u}$ was demonstrated in numerical experiments (Kritsuk *et al.* 2007*a,b*) and independently verified in a number of numerical studies (Kowal & Lazarian 2007; Schmidt *et al.* 2008; Federrath *et al.* 2010; Price & Federrath 2010; Schwarz *et al.* 2010), suggesting, by dimensional arguments, the presence of an inertial cascade. More recently, analytical scaling relations for compressible turbulence were derived and analyzed (Falkovich *et al.* 2010; Galtier & Banerjee 2011; Wagner *et al.* 2012; Banerjee & Galtier

---

† Email address for correspondence: akritsuk@ucsd.edu

2013) and the existence of an intermediate scaling range dominated by inertial dynamics was demonstrated rigorously based on coarse-graining (Aluie 2011; Aluie *et al.* 2012; Aluie 2013). This contribution reports on the verification of the new relation presented in Galtier & Banerjee (2011) with data from a Mach 6 simulation (Kritsuk *et al.* 2007*a*) and on the phenomenology that follows from these results.

2. A fourth-order relation

Consider a system of Navier–Stokes equations for an isothermal compressible fluid in three dimensions

$$\partial_t \rho + \boldsymbol{\nabla} \cdot (\rho \boldsymbol{u}) = 0, \tag{2.1}$$

$$\partial_t (\rho \boldsymbol{u}) + \boldsymbol{\nabla} \cdot (\rho \boldsymbol{u} \boldsymbol{u}) + \boldsymbol{\nabla} p = \eta \Delta \boldsymbol{u} + \frac{\eta}{3} \boldsymbol{\nabla} (\boldsymbol{\nabla} \cdot \boldsymbol{u}) + \boldsymbol{f}, \tag{2.2}$$

where $p = c_{\rm s}^2 \rho$ is the pressure, $c_{\rm s}$ is the speed of sound, $\eta > 0$ is the dynamic viscosity (η is constant in space and time in isothermal flows) and $\boldsymbol{f}(\boldsymbol{x}, t)$ is a random force. Besides the usual conservation of mass and momentum expressed by (2.1) and (2.2), let us mention two additional ideal integral invariants in unforced isothermal fluids: (i) the total energy density,

$$\langle E \rangle \equiv \langle \rho u^2 / 2 + \rho e \rangle, \tag{2.3}$$

where $e = c_{\rm s}^2 \ln(\rho/\rho_0)$ is the specific isothermal compressive potential energy, ρ_0 is the mean density of the fluid and angle brackets $\langle \ldots \rangle$ in this context indicate average over the volume of the fluid, $\frac{1}{V} \int_V (\ldots) \mathrm{d}V$; and (ii) the mean kinetic helicity,

$$\langle H \rangle \equiv \langle \boldsymbol{u} \cdot \boldsymbol{\omega} \rangle / 2, \tag{2.4}$$

where $\boldsymbol{\omega} \equiv \boldsymbol{\nabla} \times \boldsymbol{u}$ is the vorticity. In the forced system, the evolution of total energy density is determined by the balance between the action of large-scale force and small-scale viscous dissipation

$$\partial_t \langle E \rangle = \langle \epsilon \rangle - \eta \left\langle \omega^2 - 4d^2/3 \right\rangle, \tag{2.5}$$

where $\epsilon \equiv \boldsymbol{u} \cdot \boldsymbol{f}$ is the local energy injection rate and $d \equiv \boldsymbol{\nabla} \cdot \boldsymbol{u}$ is the dilatation.

Assuming that a statistical steady state exists at $Re \gg 1$, the following relation for homogeneous turbulence in the inertial interval can be derived (Galtier & Banerjee 2011)

$$\langle d' \left(R - 2E - p \right) + d \left(R' - 2E' - p' \right) \rangle + \boldsymbol{\nabla_r} \cdot \left\langle \left[\delta(\rho \boldsymbol{u}) \cdot \delta \boldsymbol{u} + 2\delta \rho \delta e \right] \delta \boldsymbol{u} + \tilde{\delta} e \delta(\rho \boldsymbol{u}) \right\rangle = -4\varepsilon, \tag{2.6}$$

note a different pressure-dilatation term placement (Banerjee & Galtier 2013). Here $\delta \boldsymbol{q}(r) \equiv \boldsymbol{q}(\boldsymbol{x}') - \boldsymbol{q}(\boldsymbol{x})$ is the increment in quantity $\boldsymbol{q}$ corresponding to the increment $\boldsymbol{r} = \boldsymbol{x}' - \boldsymbol{x}$, $r \equiv |\boldsymbol{r}|$, $R \equiv \rho \boldsymbol{u} \cdot \boldsymbol{u}' + 2\rho e'$, $R' \equiv \rho' \boldsymbol{u}' \cdot \boldsymbol{u} + 2\rho' e$, $\tilde{\delta} q \equiv q' + q$, $\boldsymbol{\nabla_r} \equiv \hat{\mathbf{e}}_i \partial/\partial r_i$ denotes partial derivatives with respect to the increment $\boldsymbol{r}$, $\hat{\mathbf{e}} = \{\hat{\mathbf{e}}_1, \hat{\mathbf{e}}_2, \hat{\mathbf{e}}_3\}$ is an orthonormal basis,

$$\varepsilon = \langle \boldsymbol{u}' \cdot \boldsymbol{f} + \boldsymbol{u} \cdot \boldsymbol{f}' + \boldsymbol{u}' \cdot \boldsymbol{f} \rho'/\rho + \boldsymbol{u} \cdot \boldsymbol{f}' \rho/\rho' \rangle / 4 \tag{2.7}$$

is the mean energy density injection rate and $\langle \ldots \rangle$ denote an ensemble-average.

Equation (2.6) can be written in symbolic form as

$$S(r) + \boldsymbol{\nabla_r} \cdot \boldsymbol{F} = -4\varepsilon, \tag{2.8}$$

where $\boldsymbol{F}(r)$ is the total energy flux vector and $S(r)$ represents 'source' terms on the left-hand side of (2.6) that depend on the potential component of the velocity and can be

expressed via increments

$$S(r) = \left\langle \left[\delta(d\rho \boldsymbol{u}) - \tilde{\delta} d\delta(\rho \boldsymbol{u}) \right] \cdot \delta\boldsymbol{u} + 2 \left[\delta(d\rho) - \tilde{\delta} d\delta\rho \right] \delta e + \delta d \delta p - 2 dp \right\rangle. \qquad (2.9)$$

On the basis of empirical evidence (see § 3 below), in supersonic turbulence the pressure-dilatation contribution to the source at $r = 0$ is positive, $S(0) = -2\langle dp \rangle > 0$. Since both e and p are proportional to c_s^2, only the first term in (2.9) will contribute to $S(r)$ at high Mach numbers ($c_s \to 0$)

$$S(r) \approx \mathscr{S}(r) \equiv \left\langle [\delta(d\rho \boldsymbol{u}) - \tilde{\delta} d \, \delta(\rho \boldsymbol{u})] \cdot \delta\boldsymbol{u} \right\rangle \qquad (2.10)$$

(cf. equation (16) in Galtier & Banerjee 2011). Vector relation (2.8) should be compared to a primitive form of Kolmogorov's (1941) exact and nontrivial four-fifths law,

$$\rho_0 \boldsymbol{\nabla_r} \cdot \langle (\delta\boldsymbol{u})^2 \delta\boldsymbol{u} \rangle = -4\varepsilon \qquad (2.11)$$

(e.g. Frisch 1995, equation (6.8)), which follows from (2.6), assuming incompressibility.

If the force in (2.2) is expressed in terms of the external acceleration, $\boldsymbol{f} \equiv \rho\boldsymbol{a}$, then

$$\varepsilon = \langle \rho \boldsymbol{u}' \cdot \boldsymbol{a} + \rho' \boldsymbol{u} \cdot \boldsymbol{a}' + \rho' \boldsymbol{u}' \cdot \boldsymbol{a} + \rho \boldsymbol{u} \cdot \boldsymbol{a}' \rangle / 4. \qquad (2.12)$$

In isotropic turbulence,

$$\varepsilon = \langle \rho \boldsymbol{u}' \cdot \boldsymbol{a} + \rho' \boldsymbol{u}' \cdot \boldsymbol{a} \rangle / 2 = \langle \tilde{\delta} \rho \, (\boldsymbol{u}' \cdot \boldsymbol{a}) \rangle / 2. \qquad (2.13)$$

For incompressible fluids, it can be shown that $\varepsilon(r) = \rho_0 \langle \boldsymbol{u}' \cdot \boldsymbol{a} \rangle \approx \rho_0 \langle \boldsymbol{u} \cdot \boldsymbol{a} \rangle \equiv \rho_0 \bar{\varepsilon}$, if the acceleration $\boldsymbol{a}(\boldsymbol{x}, t)$ (and hence the force $\rho_0 \boldsymbol{a}$) operate at large scales only. Here, $\bar{\varepsilon}$ denotes the (constant) average energy injection rate per unit mass.

This conventional technique, however, cannot be carried over to compressible fluid turbulence. In the limit of large correlation length L_a of the acceleration $\boldsymbol{a}$, for $r \ll L_a$ the second term in (2.13) can be reduced to a constant $\langle \rho' \boldsymbol{u}' \cdot \boldsymbol{a} \rangle \approx \langle \rho \boldsymbol{u} \cdot \boldsymbol{a} \rangle$, while the first cannot. If the force $\boldsymbol{f}(\boldsymbol{x}, t)$ had a large correlation length L_f instead, the first term in (2.13) would reduce to the same combination $\langle \rho \boldsymbol{u}' \cdot \boldsymbol{a} \rangle = \langle \boldsymbol{u}' \cdot \boldsymbol{f} \rangle \approx \langle \boldsymbol{u} \cdot \boldsymbol{f} \rangle = \langle \rho \boldsymbol{u} \cdot \boldsymbol{a} \rangle$ for $r \ll L_f$, but the second could not be decoupled simultaneously. On the basis of (2.13), in supersonic turbulence the large-scale external force assumption is incompatible with the presence of inertial interval due to strong density variations on all scales (see also Wagner *et al.* 2012). If the large-scale acceleration is also short-correlated in time, then the density can be decoupled for r in the inertial interval $\langle \rho \boldsymbol{u}' \cdot \boldsymbol{a} \rangle \approx \langle \rho \rangle \langle \boldsymbol{u} \cdot \boldsymbol{a} \rangle$ (e.g. Wagner *et al.* 2012). In this case, (2.13) would reduce to

$$\varepsilon \approx \rho_0 \langle \boldsymbol{u} \cdot \boldsymbol{a} \rangle = \rho_0 \bar{\varepsilon} = \text{const.} \qquad (2.14)$$

In reality, the large-scale acceleration (e.g. the free-fall acceleration in turbulent convection) is often not short-correlated in time. Also in simulations, forcing is routinely employed to mimic the energy cascade incoming from scales larger than the box size; thus the correlation time cannot be shorter than the large eddy turnover time and it is hard to expect the decoupling in the form of (2.14).

Nevertheless, the density field in supersonic turbulence has a very short correlation length $L_\rho \ll L_u \ll L_a$. Since $\boldsymbol{u}$ and $\boldsymbol{a}$ are larger-scale fields, while ρ related to the velocity gradient is a small-scale quantity controlled by the nonlinearity of governing equations (2.1) and (2.2), one can expect that $\langle \rho \boldsymbol{u}' \cdot \boldsymbol{a} \rangle \approx \langle \rho' \boldsymbol{u}' \cdot \boldsymbol{a} \rangle \approx \langle \rho \boldsymbol{u} \cdot \boldsymbol{a} \rangle$. Hence, even for $\boldsymbol{a}$ with a finite correlation time, the approximation

$$\varepsilon(r) \approx \langle \rho \boldsymbol{u} \cdot \boldsymbol{a} \rangle = \varepsilon_0 \qquad (2.15)$$

is justified for $L_\rho \lesssim r \ll L_a$. Using a different approach based on coarse-graining, Aluie
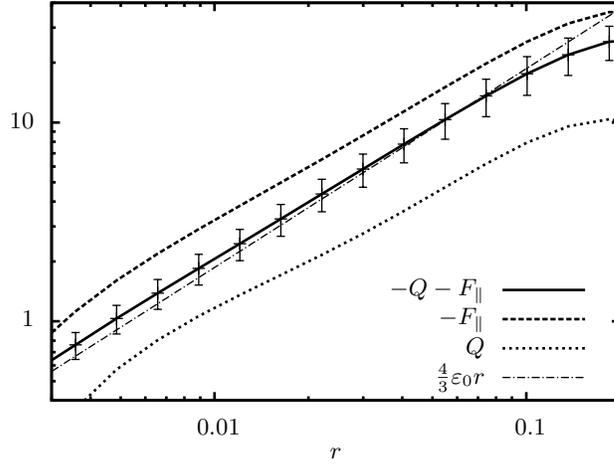
FIGURE 1. Time-average scaling for the left-hand side and right-hand side of (2.16), including individual contributions from the flux and source terms. Note that $F_\parallel(r) < 0$ (direct energy cascade) and $S(r) > 0$ (effective additional energy injection). Error bars indicate $\pm 1\sigma$ variation of the left-hand side of (2.16) in our sample of 86 flow snapshots.

(2013) rigorously proved that the energy injection rate is constant at scales sufficiently separated from the injection scale, if the external acceleration used to support a statistical steady state is restricted to large scales. We will show how well (2.14) and (2.15) hold in § 3.

For now, however, let us assume $\varepsilon(r) = \varepsilon_0$ and integrate (2.8) over a ball of radius r, to obtain an approximate scalar relation for isotropic turbulence in symbolic form:

$$Q(r) + F_\parallel(r) \simeq -\frac{4}{3}\varepsilon_0 r, \tag{2.16}$$

where the source function

$$Q(r) \equiv \frac{1}{r^2}\int_0^r S(r)r^2\mathrm{d}r \tag{2.17}$$

and the longitudinal flux of total energy

$$F_\parallel(r) \equiv \boldsymbol{F}\cdot\boldsymbol{r}/r = \left\langle [\delta(\rho\boldsymbol{u})\cdot\delta\boldsymbol{u} + 2\delta\rho\delta e]\,\delta u_\parallel + \tilde{\delta}e\delta(\rho u_\parallel)\right\rangle. \tag{2.18}$$

The inertial part of the flux dominates at high Mach numbers ($c_\mathrm{s} \to 0$):

$$F_\parallel(r) \approx \mathscr{F}_\parallel(r) \equiv \left\langle\delta(\rho\boldsymbol{u})\cdot\delta\boldsymbol{u}\,\delta u_\parallel\right\rangle \tag{2.19}$$

– see also (2.10). While approximation (2.19) does not include the flux of compressive energy density ρe, compressibility is still partly accounted for by the momentum difference $\delta(\rho\boldsymbol{u})$. Also note that $F_\parallel(0) = 0$, $\mathscr{F}_\parallel(0) = 0$ and $Q(0) = 0$.

3. Numerical verification

To evaluate (2.16), we shall use data from a numerical experiment designed to study the inertial range statistics of supersonic homogeneous isotropic turbulence (Kritsuk *et al.* 2007*a*). The simulation was carried out following the traditional implicit large eddy simulation (ILES) approach to the modeling of turbulent flows with strong shocks (Grinstein *et al.* 2007), using an implementation of the piecewise parabolic method (PPM,
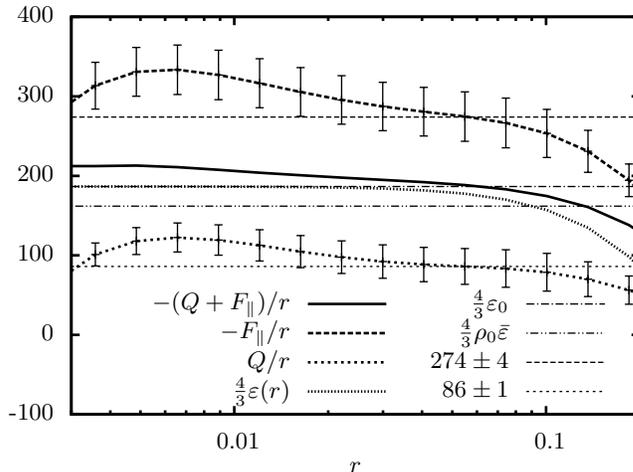
FIGURE 2. Compensated scaling for the flux and source terms from (2.16). Also shown are various proxies for the energy injection rate, including the two-point momentum–acceleration and velocity–force correlation functions, as well as single-point averages with and without density-weighting. Error bars indicate $\pm 1\sigma$ variation of the flux and source terms in our sample.

Colella & Woodward 1984) in the Enzo code (O'Shea *et al.* 2004). The forced Euler equations for an isothermal fluid with the mean density $\rho_0 = 1$ were numerically integrated in a cubic periodic domain with a linear size $L = 1$ covered by a uniform Cartesian grid of 1024^3 cells. The turbulent r.m.s. Mach number, $M \sim 6$, and a steady rate of the kinetic energy injection were maintained by a random large-scale acceleration field, $\boldsymbol{a}(\boldsymbol{x}, t) = C(t)\boldsymbol{a}_0(\boldsymbol{x})$, with power limited to wavenumbers $k/k_{\min} \in [1, 2]$, where $k_{\min} = 2\pi/L$. The spatially fixed external acceleration $\boldsymbol{a}_0(\boldsymbol{x})$ was normalized at every time step to keep the energy injection rate approximately constant in time, $\varepsilon_0 = 140$; the normalization factor $C(t)$ had a standard deviation of $\sim 5\%$ during the simulation. For this work, we used a subset of 86 full data snapshots evenly distributed in the range $t/\tau \in [6, 10]$, where the flow crossing time $\tau \equiv L/(2c_{\mathrm{s}}M) \simeq 0.08$. For each snapshot, we computed $\bar{\varepsilon}$ and evaluated $S(r)$, $Q(r)$, $F_{\|}(r)$, and $\varepsilon(r) = \langle \tilde{\delta}\rho\,(\boldsymbol{u}' \cdot \boldsymbol{a}) \rangle / 2$ for 16 discrete values of increment r from the interval $r/\Delta \in [8, 128]$, where Δ is the grid spacing, using $2^{31} \approx 2 \times 10^9$ randomly selected point pairs for each value of r.

Figure 1 compares the scaling of $-(Q + F_{\|})$ with the analytical prediction $4\varepsilon_0 r/3$, indicating that the approximate relation (2.16) holds reasonably well. Also shown are individual contributions for Q and $F_{\|}$. As expected for direct energy cascade, the flux is negative across the inertial interval. The source function is positive and a factor of ≈ 3.2 smaller than the flux. It represents the net effect of mean dilatation at scale r (conditioned on the energy density at this scale) on the associated energy flux. The source can be understood as a (positive) correction to ε_0, associated with the evolving metric in parts of the volume that are subject to compression. In a different context, such 'adiabatic heating' of compressible turbulent fluids was recently considered by Robertson & Goldreich (2012).

Figure 2 provides more detail by showing compensated scaling of various terms in (2.16); note that the inertial sub-range is limited to $r \in [0.03, 0.1]$ (Kritsuk *et al.* 2007*a*). On smaller scales, a bump indicating possible bottleneck contamination is clearly visible; on larger scales, the action of force is felt directly and $\varepsilon(r)$ starts to decline. The energy injection rate ε_0 defined in (2.15) gives an accurate measure for $\varepsilon(r) \approx 140$ in the inertial interval, while (2.14), which ignores the density–velocity correlation, underestimates
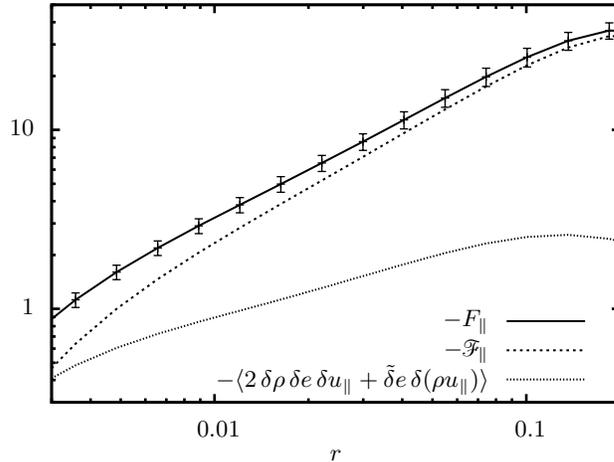
FIGURE 3. Scaling of the longitudinal flux of total, kinetic and compressive energy. At $M \simeq 6$, the kinetic energy flux strongly dominates over compressive flux terms. The exponents of the least-squares fits for $r \in [0.03, 0.08]$ are 0.91 ± 0.01, 0.99 ± 0.01 and 0.44 ± 0.02 for the total, kinetic and compressive fluxes, respectively. Error bars indicate $\pm 1\sigma$ variation of the total flux.

the injection rate by $\sim 15\%$. The inertial range levels of the flux and source terms, -274 ± 4 and 86 ± 1 respectively, are estimated from the least-squares fits. The source terms play a relatively minor role across the inertial range; both individual flux and source contributions in (2.16) scale roughly linearly with r, indicating that $S(r) \approx$ const. This in turn implies that the kinetic energy cascades conservatively without substantial scale-dependent 'leakage' to the compressive potential energy (see also Aluie *et al.* 2012).

Figure 3 presents an analysis of different components of the flux in (2.18). A contribution from the inertial term $\mathscr{F}_{\parallel}$ dominates strongly on all scales, as predicted by (2.19). Two other terms related to the compressive energy flux are subdominant in the inertial range. The last term in (2.18) is ~ 1.6 dex smaller than the second.

Figure 4 shows various constituents of $S(r)$ listed in (2.9). As suggested by (2.10), the dominant contribution comes from dynamic-pressure-dilatation terms proportional to $\delta \boldsymbol{u}$; it is positive in a wide range of r and approximately constant ($\pm 4\%$) at $r \in [0.006, 0.1]$. Source terms associated with the specific compressive energy difference δe contribute positively on small scales $r \lesssim 0.03$ and act as a sink at $r \gtrsim 0.03$. While their effect on the inertial range is minimal, they are responsible for an $\approx 40\%$ excess in $S(r)$ centered around $r \simeq 0.004$. The resulting small-scale excess in positive $S(r)$ is in turn responsible for the excess in negative $F_{\parallel}(r)$ (see figure 2). The impact of pressure-dilatation terms $\langle \delta d \delta p - 2 dp \rangle$ on $S(r)$ is minor and they can be ignored in the inertial range. As $r \to 0$, the source is finite and positive: $S(r) \to -2\langle dp \rangle \simeq 73$. The average pressure dilatation may depend on various factors such as the Mach number, adopted equation of state, numerical resolution and so on. While for isothermal turbulence at $M \sim 6$ we obtain $\langle dp \rangle / (\gamma M^2) \approx -1$, also negative but substantially smaller ($\lesssim 0.04$) absolute values are reported by Aluie *et al.* (2012) and Wang *et al.* (2012) for ideal gas models at $M \lesssim 1$. At high Mach numbers, the p.d.f. of dilatation is strongly skewed towards negative values, making the average pressure dilatation finite and negative.

Since approximations (2.10) and (2.19) hold at $M \gg 1$, (2.16) can be reduced to

$$\mathscr{Q}(r) + \mathscr{F}_{\parallel}(r) \simeq -\frac{4}{3}\mathscr{C}\varepsilon_0 r, \qquad (3.1)$$
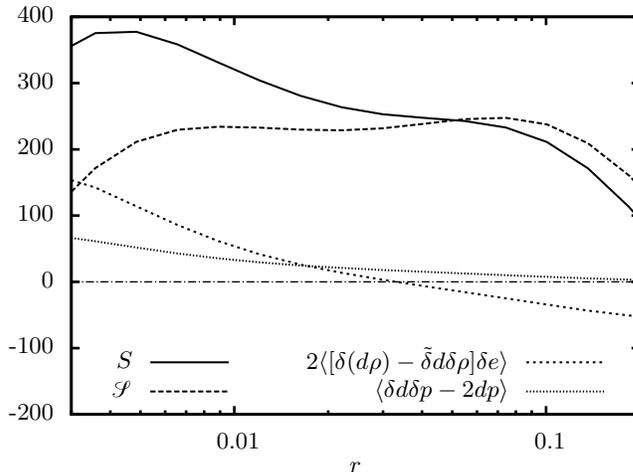
FIGURE 4. Time-average scaling of various source terms in (2.9) and (2.10).

where the source function $\mathscr{Q}(r) \equiv r^{-2} \int_0^r \mathscr{S}(r) r^2 \mathrm{d}r$ is analogous to (2.17) and $\mathscr{C} < 1$ is a constant of order unity accounting for the fraction of injected kinetic energy that goes into excitation of compressive modes that were ignored in (2.10) and (2.19). Figure 5 illustrates the quality of approximations at $M \simeq 6$, where $\mathscr{C} \simeq 0.84$, i.e. $\approx 16\%$ of the energy input supports modes related to the compressive energy and pressure dilatation. Note that at $M \simeq 6$ the right-hand side of (3.1) can be replaced by the incompressible expression $-4\rho_0 \bar{\varepsilon}/3$ without substantial loss of accuracy: see (2.14) for the definition of $\bar{\varepsilon}$. As $\mathscr{S}(r) \approx \mathscr{S}_0$ is nearly constant in the inertial interval, $\mathscr{F}_\parallel(r) \simeq -4\varepsilon_\mathrm{eff} r/3$, where $\varepsilon_\mathrm{eff} = \mathscr{C}\varepsilon_0 + \mathscr{S}_0/4$.

4. Discussion

In practical astrophysical applications, where order-of-magnitude estimates are considered sufficient, relation (3.1) can be more convenient than (2.16). We therefore explored the scaling of several proxies to $\mathscr{F}_\parallel$, which are more closely related to observables and to structure functions previously measured numerically. Figure 6 illustrates the scaling of $\mathscr{F}_\parallel(r)$ as well as that of the transverse $\langle|\delta v_\perp|^3\rangle$ and longitudinal $\langle|\delta v_\parallel|^3\rangle$ structure functions of the mass-weighted velocity and compares these with theoretical expectations based on (2.16) and (3.1). The inertial range slopes of these proxies are close to linear, so they provide a convenient way of estimating the value of the total flux $F_\parallel$ and thereby the kinetic energy injection rate ε_0.

Figure 6 shows that $\mathscr{F}_\parallel(r) \sim 1.7\varepsilon_0$. The total energy flux $F_\parallel$ would have an 18% larger offset, corresponding to a factor of 2. The proxies based on the longitudinal and transverse structure functions of $\boldsymbol{v}$ overestimate ε_0 by factors 3.5 and 4.1, respectively. These values can be used to estimate the energy injection rate required to sustain turbulent cascade in the interstellar medium of the Milky Way (Hennebelle & Falgarone 2012).

An interesting feature to notice in figures 5 and 6 is the extended (~ 1 dex) linear scaling range of $\mathscr{F}_\parallel$, which continues down to $r \simeq 0.008 \simeq 8\Delta$. In ILES carried out with a PPM-based code, all scales below $\sim 16\Delta$ are strongly affected by numerical dissipation (Porter & Woodward 1994). Scales shorter than $\sim 32\Delta$ are usually identified with the so-called 'bottleneck bump' (Falkovich 1994; Porter *et al.* 1994), where the energy piles up
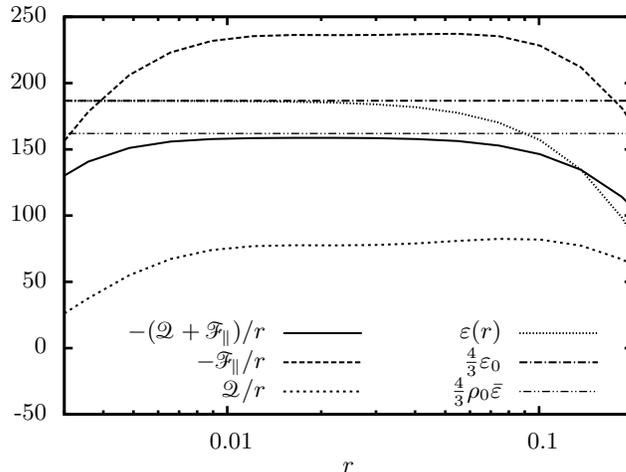
FIGURE 5. As figure 2, but for the flux and source terms from an approximate relation (3.1).

in the near-dissipation part of the inertial range due to a steep wavenumber dependence of numerical diffusivity in the dissipation range ($\propto k^{4-5}$ for PPM, see Porter *et al.* 1992). Similar bumps are present in the spectra of velocity, density and various mixed quantities in supersonic turbulence (Kritsuk *et al.* 2007a). In structure functions, the bottleneck is expected to be more pronounced at higher orders (Falkovich 1994); it is also less localized than in power spectra due to mixing of small- and large-scale information (Dobler *et al.* 2003; Davidson & Pearson 2005, see, e.g., a plot of $\langle|\delta v_\perp|^3\rangle$ in figure 6 and note that we take an absolute value). The inertial flux $\mathscr{F}_\parallel$, however, does not show a bump, as expected in the inertial cascade, when an absolute value operation is not applied.

As we discussed above, the bump in the total flux is associated with the compressive energy flux contribution $\langle 2\delta\rho\delta e\delta u_\parallel\rangle$, which becomes comparable to the kinetic energy flux and also somewhat flattens below the sonic scale at $r \lesssim r_s$: $\delta u_\parallel(r_s) = c_s$. This behaviour may depend on the details of the shock-capturing scheme. Indeed, a PPM implementation in the Enzo code (O'Shea *et al.* 2004) produces a growing fraction of dilatational modes in the velocity power spectrum on scales below 32Δ (see figure 1b in Kritsuk *et al.* 2010), which could potentially contribute to the bump build-up.

5. Conclusions and final remarks

We verified a relation for correlation functions in compressible isothermal turbulence (Galtier & Banerjee 2011) with data from a numerical simulation at Mach 6 (Kritsuk *et al.* 2007a). While an isotropic version of the relation is not strictly exact, it provides a good approximation to numerical results. Our analysis of different terms in (2.16) supports a Kolmogorov-like picture of the energy cascade in supersonic turbulence previously discussed on a phenomenological level (Kritsuk *et al.* 2007a) and recently supported theoretically (Aluie 2011; Aluie *et al.* 2012; Aluie 2013). A non-trivial new approximate relation (3.1) that holds at high turbulent Mach numbers is proposed. The relation represents an important step beyond phenomenology, as it sheds light on the problem of universality in compressible turbulence and provides a way to quantitatively predict the energy injection rate from the scaling of certain combinations of observables. This result can have important implications for interstellar turbulence, as approximately constant
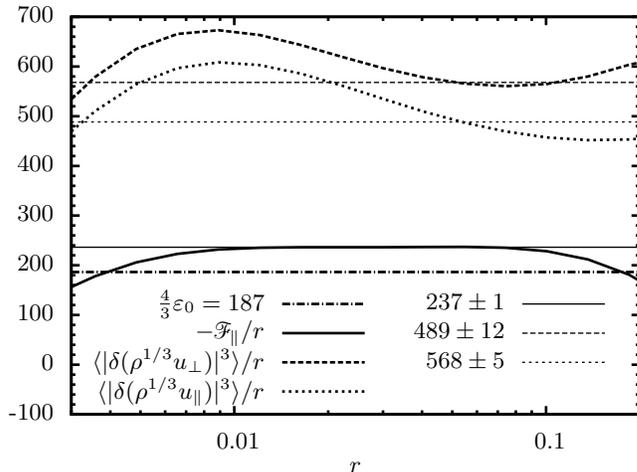
FIGURE 6. Compensated scaling for various proxies of the energy injection rate ε_0. Thin lines show horizontal least-squares fits at $r \in [0.03, 0.1]$; numbers indicate the best-fit value and its standard deviation.

energy transfer rates are observed in the ISM over more than four decades in length scale (Hennebelle & Falgarone 2012).

The fourth-order scaling relation (2.16) traditionally formulated in terms of the energy flux is not the only compressible analogue of Kolmogorov's four-fifths law. Another approximate relation for homogeneous isothermal turbulence, formulated in terms of fluxes and densities of conserved quantities,

$$\boldsymbol{\nabla_r} \cdot \left\langle \rho\rho' \left[(\boldsymbol{u} \cdot \boldsymbol{u'}) \, \boldsymbol{u'} + c_{\mathrm{s}}^2 \boldsymbol{u} \right] \right\rangle \sim - \left\langle \rho\rho' \right\rangle \bar{\varepsilon}, \tag{5.1}$$

cf. (2.6), has recently been obtained and verified with the same numerical data (Wagner *et al.* 2012). More strictly, this fifth-order flux relation should be viewed as an anisotropic analogue of the von Kármán–Howarth relation, as it involves correlation functions, but (5.1) can also be reduced to the four-fifths law in the incompressible limit (Falkovich *et al.* 2010). Note that the dependence of the density autocorrelation function in the right-hand side of (5.1) on the increment r varies with the Mach number, as does the slope of the density power spectrum (Kim & Ryu 2005). Unlike (2.16), an isotropic version of (5.1) does not have a trivial right-hand side universally linear in r. In a particular case at $M \simeq 6$, the density autocorrelation function has a logarithmic dependence on r and a closed-form analytical representation of the isotropic flux relation is feasible (see (3.3) in Wagner *et al.* 2012).

We thus conclude that at least two compressible analogues of Kolmogorov's four-fifths law exist, consistent with the extension of the turbulent energy cascade picture to supersonic regimes. Only the fourth-order energy cascade relation (2.16) is 'universal' in the sense that its right-hand side remains approximately linear in the inertial range at all Mach numbers. It is worth noting that the fourth-order relation exploits the conservation of total energy (which is an inviscid invariant), while the fifth-order one follows from conservation of momentum and involves the momentum density and flux.

REFERENCES

ALUIE, H. 2011 Compressible turbulence: The cascade and its locality. *Phys. Rev. Lett.* **106** (17), 174502.

ALUIE, H. 2013 Scale decomposition in compressible turbulence. *Physica D* **247** (1), 54–65.

ALUIE, H., LI, S. & LI, H. 2012 Conservative cascade of kinetic energy in compressible turbulence. *Astrophys. J. Lett.* **751**, L29.

BANERJEE, S. & GALTIER, S. 2013 Exact relation with two-point correlation functions and phenomenological approach for compressible magnetohydrodynamic turbulence. *Phys. Rev. E* **87**, 013019.

COLELLA, P. & WOODWARD, P. R. 1984 The piecewise parabolic method (PPM) for gas-dynamical simulations. *J. Comput. Phys.* **54**, 174–201.

DAVIDSON, P. A. & PEARSON, B. R. 2005 Identifying turbulent energy distributions in real, rather than fourier, space. *Phys. Rev. Lett.* **95** (21), 214501.

DOBLER, W., HAUGEN, N. E., YOUSEF, T. A. & BRANDENBURG, A. 2003 Bottleneck effect in three-dimensional turbulence simulations. *Phys. Rev. E* **68** (2), 026304.

FALKOVICH, G. 1994 Bottleneck phenomenon in developed turbulence. *Phys. Fluids* **6**, 1411–1414.

FALKOVICH, G., FOUXON, I. & OZ, Y. 2010 New relations for correlation functions in Navier-Stokes turbulence. *J. Fluid Mech.* **644**, 465–472.

FEDERRATH, C., ROMAN-DUVAL, J., KLESSEN, R. S., SCHMIDT, W. & MAC LOW, M.-M. 2010 Comparing the statistics of interstellar turbulence in simulations and observations. Solenoidal versus compressive turbulence forcing. *Astron. Astrophys.* **512**, A81.

FRISCH, U. 1995 *Turbulence. The legacy of A. N. Kolmogorov*. Cambridge University Press, Cambridge.

GALTIER, S. & BANERJEE, S. 2011 Exact relation for correlation functions in compressible isothermal turbulence. *Phys. Rev. Lett.* **107** (13), 134501.

GRINSTEIN, F. F., MARGOLIN, L. G. & RIDER, W. J., ed. 2007 *Implicit Large Eddy Simulation: Computing Turbulent Fluid Dynamics*. Cambridge University Press, Cambridge.

HENNEBELLE, P. & FALGARONE, E. 2012 Turbulent molecular clouds. *Astron. Astrophys. Rev.* **20:55**, 1–58.

HOBBS, A., NAYAKSHIN, S., POWER, C. & KING, A. 2011 Feeding supermassive black holes through supersonic turbulence and ballistic accretion. *Mon. Not. Roy. astron. Soc.* **413**, 2633–2650.

INGENITO, A. & BRUNO, C. 2010 Physics and regimes of supersonic combustion. *AIAA Journal* **48**, 515–525.

KIM, J. & RYU, D. 2005 Density power spectrum of compressible hydrodynamic turbulent flows. *Astrophys. J. Lett.* **630**, L45–L48.

KOLMOGOROV, A. N. 1941 Dissipation of energy in the locally isotropic turbulence. *Dokl. Akad. Nauk SSSR* **32**, 19–21.

KOWAL, G. & LAZARIAN, A. 2007 Scaling relations of compressible MHD turbulence. *Astrophys. J. Lett.* **666**, L69–L72.

KRITSUK, A. G., NORMAN, M. L., PADOAN, P. & WAGNER, R. 2007*a* The statistics of supersonic isothermal turbulence. *Astrophys. J.* **665**, 416–431.

KRITSUK, A. G., PADOAN, P., WAGNER, R. & NORMAN, M. L. 2007*b* Scaling laws and intermittency in highly compressible turbulence. In *Turbulence and Nonlinear Processes in Astrophysical Plasmas* (eds. D. Shaikh & G. P. Zank), *AIP Conf. Proc.* **932**, 393–399.

KRITSUK, A. G., USTYUGOV, S., NORMAN, M. L. & PADOAN, P. 2010 Self-organization in turbulent molecular clouds: Compressional versus solenoidal modes. In *Numerical Modeling of Space Plasma Flows* (eds. N. Pogorelov, E. Audit, G. Zank), *ASP Conf. Ser.* **429**, 15–21.

MOFFAT, A. F. J. & ROBERT, C. 1994 Clumping and mass loss in hot star winds. *Astrophys. J.* **421**, 310–313.

OGDEN, D. E., GLATZMAIER, G. A. & WOHLETZ, K. H. 2008 Effects of vent overpressure on

buoyant eruption columns: Implications for plume stability. *Earth and Planetary Sci. Lett.* **268**, 283–292.

O'SHEA, B. W., BRYAN, G., BORDNER, J., NORMAN, M. L., ABEL, T., HARKNESS, R. & KRITSUK, A. 2004 Introducing Enzo, an AMR cosmology application. *ArXiv* (astro-ph/0403044).

PAN, L., PADOAN, P. & KRITSUK, A. G. 2009 Dissipative structures in supersonic turbulence. *Phys. Rev. Lett.* **102**, 034501.

PORTER, D. H., POUQUET, A. & WOODWARD, P. R. 1992 A numerical study of supersonic turbulence. *Theor. Comput. Fluid Dyn.* **4**, 13–49.

PORTER, D. H., POUQUET, A. & WOODWARD, P. R. 1994 Kolmogorov-like spectra in decaying three-dimensional supersonic flows. *Phys. Fluids* **6**, 2133–2142.

PORTER, D. H. & WOODWARD, P. R. 1994 High-resolution simulations of compressible convection using the piecewise-parabolic method. *Astrophys. J. Suppl.* **93**, 309–349.

PRICE, D. J. & FEDERRATH, C. 2010 A comparison between grid and particle methods on the statistics of driven, supersonic, isothermal turbulence. *Mon. Not. Roy. astron. Soc.* **406**, 1659–1674.

ROBERTSON, B. & GOLDREICH, P. 2012 Adiabatic Heating of Contracting Turbulent Fluids. *Astrophys. J. Lett.* **750**, L31.

SCHMIDT, W., FEDERRATH, C. & KLESSEN, R. 2008 Is the scaling of supersonic turbulence universal? *Phys. Rev. Lett.* **101** (19), 194505.

SCHWARZ, C., BEETZ, C., DREHER, J. & GRAUER, R. 2010 Lyapunov exponents and information dimension of the mass distribution in turbulent compressible flows. *Phys. Lett. A* **374**, 1039–1042.

WAGNER, R., FALKOVICH, G., KRITSUK, A. G. & NORMAN, M. L. 2012 Flux correlations in supersonic isothermal turbulence. *J. Fluid Mech.* **713**, 482–490.

WANG, J., SHI, Y., WANG, L.-P., XIAO, Z., HE, X. & CHEN, S. 2012 Effect of compressibility on the small-scale structures in isotropic turbulence. *J. Fluid Mech.*, **713**, 588–631.